Volume 321, number 2,3, 107–110 FEBS 12316 April 1993

Secondary structure of the *oct-3* POU homeodomain as determined by ^{1}H–^{15}N NMR spectroscopy

Eugene H. Morita[a], Masahiro Shirakawa[a], Fumiaki Hayashi[b], Masayoshi Imagawa[c] and Yoshimasa Kyogoku[a]

[a]*Institute for Protein Research, Osaka University, 3-2 Yamadaoka, Suita, Osaka 565, Japan,* [b]*Shionogi Research Laboratories, Shionogi & Co., Fukushima-ku, Osaka 553, Japan* and [c]*School of Pharmaceutical Sciences, Osaka University, 1-6 Yamadaoka, Suita, Osaka 565, Japan*

Received 5 February 1993

Most of the ^{1}H and ^{15}N magnetic resonances of the 66 amino acid long POU homeodomain of mouse Oct-3 have been assigned by the combined use of the two-dimensional homonuclear, and two- and three-dimensional heteronuclear NMR methods. The sequential NOE connectivities and amide proton exchange measurements indicate the presence of three helical regions within the domain. The positions of the three helices correspond well to those of other homeodomains, the three-dimensional structures of which have already been determined. The present NMR study provides the first experimental evidence for the existence of a helix-turn-helix motif in the *oct-3* POU homeodomain.

POU domain; 3D NMR; Homeodomain; Secondary structure; Oct-3

1. INTRODUCTION

During the last few years it has emerged that the DNA binding domains of most eukaryotic *trans*-acting factors have common DNA binding motifs, such as zinc-finger, helix-turn-helix, basic region-leucine zipper (bZip), helix-loop-helix and β-sheet [1]. Homeodomains having a helix-turn-helix motif were first found in many homeotic gene products of *Drosophila*, and later in many mammalian transcription factors, such as the POU family. The POU family reported by Herr et al. [2] consists of POU-specific domains (A and B domains) in addition to a POU homeodomain. The POU homeodomain is thought to have similar secondary and tertiary structures to those of other homeodomains [3]. Although other isolated homeodomains are capable of binding to a specific DNA sequence by themselves, both POU-specific and homeodomains are required for high-affinity sequence-specific DNA binding.

An octamer binding factor, Oct-3, having a POU domain as the DNA binding domain, is activated in undifferentiated embryonal carcinoma cells but is turned off upon differentiation [4]. It presumably regulates the expression of its target genes in a positive as well as a negative manner [5]. Imagawa et al. showed that both POU-specific and homeodomains are essential for high-affinity sequence-specific DNA binding [6].

Correspondence address: Y. Kyogoku, Institute for Protein Research, Osaka University, 3-2 Yamadaoka, Suita, Osaka 565, Japan. Fax: (81) (6) 876 2533.

We report here extensive ^{1}H and ^{15}N magnetic resonance assignments and secondary structure determination of the 66 amino acid long POU homeodomain of Oct-3, which has an additional methionyl residue at the N-terminus. The assignments were made by means of two- and three-dimensional heteronuclear NMR experiments, and the elucidation of the secondary structure was based mainly on short- and medium-range NOEs, and the H–^{2}H exchange rates of main chain amide protons. The present data provide evidence for the presence of a helix-turn-helix motif in this domain similar to those found in other homeodomains [7–10]. We believe that this is the first direct experimental evidence for the existence of a helix-turn-helix motif in the POU homeodomain.

2. MATERIALS AND METHODS

2.1. *Growth of bacteria and protein purification*

Recombinant *oct-3* POU homeodomain, which contained amino acid residues 217–282 of mouse Oct-3 and an additional methionyl residue at its N-terminus, was prepared with *E. coli* (strain BL-21) harboring plasmid pAR2113-POU(H) [6]. The uniformly ^{15}N labeled POU homeodomain was obtained from bacteria grown in M9 medium with $^{15}NH_4Cl$ as the sole nitrogen source.

The protein was purified by chromatography on S-Sepharose, FPLC mono-S, and Superdex75 (Pharmacia) columns. The protein was more than 95% pure, as judged by SDS polyacrylamide gel electrophoresis.

The samples for NMR measurements typically comprised 3.2 mM protein in 90% H_2O/10% $^{2}H_2O$, or in $^{2}H_2O$, containing 50 mM potassium phosphate, 50 mM KCl and 1 mM dithiothreitol, pH 5.2 (direct pH meter reading).

2.2. *NMR spectroscopy*

NMR spectra were recorded at 30°C. Two-dimensional (2D) ^{1}H–^{1}H

spectra of the unlabeled POU homeodomain were acquired with either a JEOL GSX-500 spectrometer or a Varian Unity-600 spectrometer. Homonuclear 2D DQF-COSY and NOESY spectra were typically recorded using a spectral width of 6,000 Hz in both dimensions, with 256 t_1 increments of 2K complex data points. 2D ^1H–^{15}N HSQC, ^1H–^{15}N HSQC-NOESY and ^1H–^{15}N HMQC-J spectra [11–14] of the uniformly ^{15}N-labeled POU homeodomain were recorded with a Bruker AMX-500 spectrometer. Solvent suppression was achieved by presaturation during the relaxation delay, or by the use of spin lock purge pulses [15]. ^{15}N decoupling during acquisition was achieved using GARP-1 phase modulation [16]. All 2D spectra were recorded in the pure absorption mode with t_1 quadrature detection achieved using TPPI-States [17] or the procedure of States et al. [18].

Three-dimensional (3D) TOCSY-HSQC and NOESY-HSQC spectra of the uniformly ^{15}N labeled POU homeodomain were recorded at 30°C with a Bruker AMX-500 spectrometer. The pulse sequences used were minor modifications of those previously described by Fairbrother et al. [19]. DIPSI-2 [20] was used for ^1H isotropic mixing in the 3D ^1H–^{15}N TOCSY-HSQC experiment. The isotropic mixing time in the 3D ^1H–^{15}N TOCSY-HSQC experiment was 76 ms, and the mixing time for the NOESY-HSQC experiment was 200 ms. The acquired data matrix in each 3D experiment was $128(t_1) \times 32(t_2) \times 1{,}024(t_3)$ complex points, and the spectral widths were 6,001.7, 2,027.4 and 12,500 Hz in F_1, F_2 and F_3, respectively, for the 3D TOCSY-HSQC experiment, and 6,001.7, 1,013.7 and 12,500 Hz in F_1, F_2 and F_3, respectively, for the 3D NOESY-HSQC experiment. The spectra were recorded in the pure absorption mode using TPPI-States [17] for quadrature detection in t_1 and t_2. Solvent suppression for the 3D experiments was achieved by the use of spin lock purge pulses [15].

The ^1H chemical shifts are given relative to external DSS (2,2-dimethyl-2-silapentane-5-sulfonate), and the ^{15}N chemical shifts are given relative to external 2.9 M $^{15}NH_4Cl$ in 1 M HCl and 5% ^2H_2O [21].

3. RESULTS

Almost complete assignments of the ^1H and ^{15}N resonances of the 66 residue POU homeodomain of mouse Oct-3 (residues 217–282) with an additional methionine residue at its N-terminal have been made using standard procedures. Initial spin system assignments were made on the basis of 2D homonuclear DQF-COSY and 3D ^1H–^{15}N TOCSY-HSQC spectra. Sequential assignment of the backbone ^1H and ^{15}N resonances was completed in the conventional manner [22] by mainly using 2D ^1H–^{15}N HSQC-NOESY and 3D ^1H–^{15}N NOESY-HSQC spectra to identify short-range NOEs connecting the previously identified spin-systems. The latter spectrum, together with the 3D ^1H–^{15}N TOCSY-HSQC one, was acquired using spin lock purge pulses to achieve solvent suppression, rather than presaturation, thus ensuring that the NH/$^1H\alpha$ connectivities were observed for both $^1H\alpha$ resonances close to the water signal and for the rapidly exchanging NHs. With the fairly good separation of ^{15}N chemical shift dispersion in 2D ^1H–^{15}N HSQC-NOESY, 3D ^1H–^{15}N NOESY-HSQC and 3D ^1H–^{15}N TOCSY-HSQC spectra, the sequential resonance assignment procedure was rather straightforward. Appropriate regions of the 3D NOESY-HSQC spectrum illustrating the $d_{\alpha N}$ and d_{NN} NOE connectivities are shown in Fig. 1. The side chain aromatic and NH_2 groups were assigned using the 2D homonuclear NOESY, 2D ^1H–^{15}N HSQC-NOESY and 3D ^1H–^{15}N NOESY-HSQC spectra. The details of the chemical shifts will be given elsewhere [23].

In order to determine the amide proton exchange rates of individual residues, ^1H–^{15}N HSQC spectra were acquired after dissolution of the uniformly ^{15}N-labeled

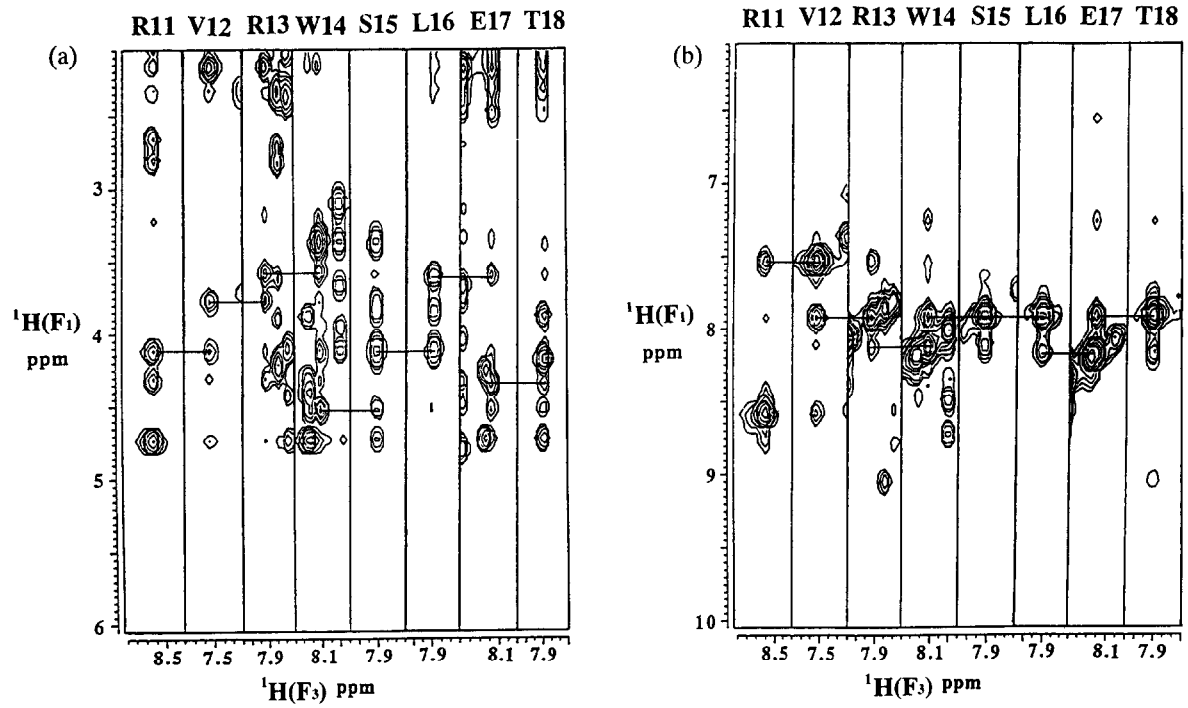

Fig. 1. Composite spectra consisting of strips taken from ^{15}N planes of 3D NOESY-HSQC spectra of the *oct-3* POU homeodomain for residues Arg^{11}–Thr^{18}. The $d_{\alpha N}(i,i+1)$ connectivities (a) and $d_{NN}(i,i+1)$ connectivities (b) are indicated by horizontal lines.

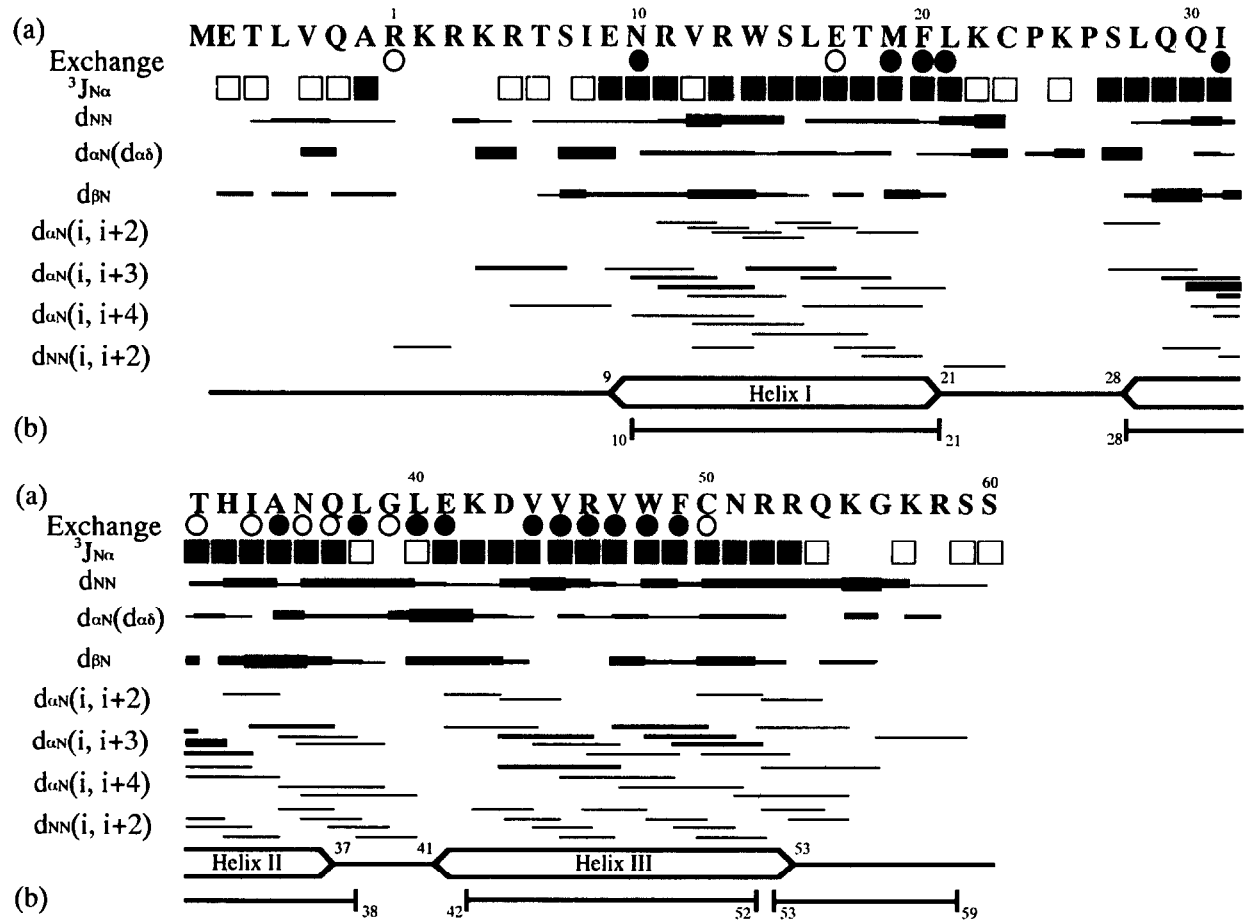

Fig. 2. (a) Summary of the sequential NOE connectivities observed for the *oct-3* POU homeodomain. Sequential NOEs are represented by bars, the height of which indicates NOE intensity (strong, medium and weak). ●, amide protons with slow exchange rates; ○, those with medium exchange rates. $^3J_{HN\alpha}$ coupling constants of less than 6.0 Hz are indicated by filled boxes, while those of greater than 7.0 Hz are indicated by open boxes. (b) Diagrammatic illustration of the secondary structure determined for the *Antennapedia* homeodomain by Qian et al. [7]. The residue numbering in (a) follows that in this reference for comparison.

POU homeodomain in ^2H_2O. The protein was lyophilized once from H_2O and then dissolved in ^2H_2O. ^1H–^{15}N HSQC spectra were acquired at 30°C at several time points starting from 7 min following dissolution. Each spectrum required 35 min acquisition time.

$^3J_{HN\alpha}$ coupling constants were determined from 2D ^1H–^{15}N HMQC-J spectrum.

The pattern of sequential and medium-range NOEs, together with the observed groupings of slow amide proton exchange and $^3J_{HN\alpha}$, are shown in Fig. 2. The residue numbering follows the scheme introduced by Qian et al. [7], to facilitate comparison of the *oct-3* POU homeodomain with other homeodomain proteins.

4. DISCUSSION

The pattern of sequential and medium-range NOEs shown in Fig. 2 strongly suggests the presence of three helical regions in the POU homeodomain of Oct-3, from residue Gln[9] to Leu[21], residue Leu[28] to Gln[37], and residue Glu[41] to Arg[53]. The observation of $^3J_{HN\text{-}H\alpha}$ coupling constants of smaller than 6 Hz also provides information concerning the boundaries of the helical regions. This was particularly useful for determining the carboxyl-terminal ends of helices II and III.

The observed grouping of amide protons with slow exchange rates is also consistent with the three helical regions. This information was also employed for defining the amino-terminal ends of helices II and III, since protection from the exchange generally begins at the fourth residue of an α-helix. The exchanging behaviors of the amide protons shown in Fig. 2 reveals that helix I is weakly protected from hydrogen exchange, relative to the other helical regions. This might suggest that helix I has a more flexible backbone structure than do helices II and III.

Another characteristic hydrogen exchange property is seen at the carboxyl-end of helix III (residues 51–53), where the exchange is considerably faster, although all the $d_{\alpha N}(i,i+3)$ connectivities were observed for the re-

gion. These data suggest that the carboxyl-end of helix III has a flexible structure or a less regular structure than a canonical α-helix. The structure perturbation of the carboxyl-terminal of the second helix of the helix-turn-helix motif was also observed in the *Antennapedia* homeodomain [7,24]. The solution structure of the *Antennapedia* homeodomain determined by Qian and coworkers has a kink at residue 52 (corresponding to Arg^{52} in the *oct-3* POU homeodomain) in the second helix of the helix-turn-helix motif, and the carboxyl-terminal region (residues 53–59) of the helix is exposed to the solvent and more flexible than the amino-terminal region of the helix (Fig. 2b) [7]. In their earlier paper describing the secondary structure of *Antennapedia* homeodomain [24], the carboxyl-terminal region (residues 53–59) of the helix was not identified as a helical region. We also did not get evidence which shows the region (residues 54–59) forms a helical structure. From the $^3J_{HN\text{-}H\alpha}$ coupling constant of Gln^{54}, it is inferred that the carboxyl-terminal of helix III is Arg^{53}.

The secondary structure of the *oct-3* POU homeodomain is similar to those of *Antennapedia* [7], *Engrailed* [8] and yeast MATα2 [9,10]. This fact strongly suggests that the POU homeodomain family has a common tertiary structure similar to other homeodomains, as predicted by Rosenfeld [3]. Botfield et al. showed that the isolated POU homeodomain of Oct-2 retains the same POU homeodomain conformation within the whole POU domain [25].

The present work demonstrates that the secondary structure of the *oct-3* POU homeodomain is similar to those of the *Antennapedia*, *Engrailed* and yeast MATα2 homeodomains. We believe that this is the first direct experimental evidence for the existence of a helix-turn-helix motif in the POU homeodomain.

Acknowledgements: This work was supported by Grants-in-Aid for Scientific Research on Priority Areas (No. 04254103) from the Ministry of Education, Science and Culture of Japan, and partly by Special Coordination Funds from the Science Technology Agency. E.H.M. was supported by JSPS Fellowships for Japanese Junior Scientists.

REFERENCES

[1] Pabo, C.O. and Sauer, R.T. (1992) Annu. Rev. Biochem. 61, 1053–1095.
[2] Herr, W., Sturm, R.A., Clere, R.G., Corcoran, L.M., Baltimore, D., Sharp, P.A., Ingraham, H.A., Rosenfeld, M.G., Finney, M., Ruvkun, G. and Horvitz, H.R. (1988) Genes Dev. 2, 1513–1516.
[3] Rosenfeld, M.G. (1991) Genes Dev. 5, 897–907.
[4] Okamoto, K., Okazawa, H., Okuda, A., Sakai, M., Muramatsu, M. and Hamada, H. (1990) Cell 60, 461–472.
[5] Okazawa, H., Okamoto, K., Ishino, F., Ishino-Kaneko, T., Takeda, S., Toyoda, Y., Muramatsu, M. and Hamada, H. (1991) EMBO J. 10, 2997–3005.
[6] Imagawa, M., Miyamoto, A., Shirakawa, M., Hamada, H. and Muramatsu, M. (1991) Nucleic Acids Res. 19, 4503–4508.
[7] Qian, Y.Q., Billeter, M., Otting, G., Mueller, M., Gehring, W.J. and Wuethrich, K. (1988) Cell 59, 573–580.
[8] Kissinger, C.R., Liu, B., Martin-Blanco, E., Kornberg, T.B. and Pabo, C.O. (1990) Cell 63, 579–590.
[9] Wolberger, C., Bershon, A.K., Liu, B., Johnson, A.D. and Pabo, C.O. (1991) Cell 67, 517–528.
[10] Phillips, C.L., Bershon, A.K., Johnson, A.D. and Dahlquist, F.W. (1991) Genes Dev. 5, 764–772.
[11] Bodenhausen, G. and Ruben, D.J. (1980) Chem. Phys. Lett. 69, 185–189.
[12] Bax, A., Ikura, M., Kay, L.E., Torchia, D.A. and Tschudin, R. (1990) J. Magn. Reson. 36, 304–318.
[13] Norwood, T.J., Boyd, J., Heritage, J.E., Sogge, N. and Campbell, I.D. (1990) J. Magn. Reson. 87, 488–501.
[14] Kay, L.E. and Bax, A. (1990) J. Magn. Reson. 86, 110–126.
[15] Messerle, B.A., Wider, G., Otting, G., Weber, C. and Wuethrich, K. (1989) J. Magn. Reson. 85, 608–613.
[16] Shaka, A.J., Barder, P.B. and Freeman, R. (1985) J. Magn. Reson. 64, 547–552.
[17] Marion, D., Ikura, M. and Bax, A. (1989) J. Magn. Reson. 84, 425–430.
[18] States, D.J., Haberkorn, R.A. and Rubren, D.J. (1982) J. Magn. Reson. 48, 286–292.
[19] Fairbrother, W.J., Cavanagh, J., Dyson, H.J., Palmer, A.G., Sutrina, S.L., Reizer, J., Saier, M.H. and Wright, P.E. (1991) Biochemistry 30, 6896–6907.
[20] Shaka, A.J., Lee, C.J. and Pines, A. (1988) J. Magn. Reson. 77, 274–293.
[21] Levy, G.C. and Lichter, R.L. (1981) Nitrogen-15 Nuclear Magnetic Resonance Spectroscopy, Wiley, New York.
[22] Wuethrich, K. (1986) NMR of Proteins and Nucleic Acids, Wiley, New York.
[23] Shirakawa, M., Morita, E.H., Hayashi, F., Imagawa, M. and Kyogoku, Y., in preparation.
[24] Otting, G., Qian, Y., Mueller, M., Affolter, M., Gehring, W. and Wuethrich, K. (1988) EMBO J. 7, 4305–4309.
[25] Botfield, M.C., Jancso, A. and Weiss, M.A. (1992) Biochemistry 31, 5841–5848.